Journal of Alloys and Compounds 470 (2009) 404–407

Contents lists available at ScienceDirect

Journal of Alloys and Compounds

journal homepage: www.elsevier.com/locate/jallcom

Stress analysis of ceramic insulation coating on Cu/MgB_2 wires for W&R MgB_2 coils

L. Arda [a,*], S. Ataoglu [b], Z. Abdulaliyev [c], O.A. Sacli [d]

[a] Faculty of Arts and Sciences, Bahcesehir University, Besiktas Campus, 34349 Besiktas, Istanbul, Turkey
[b] Division of Mechanics, Civil Engineering Department, Faculty of Civil Engineering, Istanbul Technical University, Maslak 34469, Istanbul, Turkey
[c] Metallurgical and Materials Engineering Department, Faculty of Chemical and Metallurgical Engineering, Istanbul Technical University, Maslak 34469, Istanbul, Turkey
[d] Arel University, Sefakoy – Kucukcekmece 34295, Istanbul, Turkey

ARTICLE INFO

Article history:
Received 30 December 2007
Received in revised form 15 February 2008
Accepted 22 February 2008
Available online 9 April 2008

Keywords:
Superconductors
Sol–gel processes
Elasticity
Thermal analysis

ABSTRACT

Ceramic insulation coatings were produced on Cu/MgB_2 wires, which were fabricated by Hyper Tech Research Inc., using Continuous Tube Forming and Filling (CTFF) process, from the solution of Zr, and Y based organometalic compounds, solvent and chelating agent using reel-to-reel sol–gel technique for MgB_2 coils. Y_2O_3–ZrO_2/Cu/MgB_2 wires were annealed at 700 °C for 30 min with 5.8 °C/min heating rate under 4% H_2–Ar gas flow. Residual stresses were examined for Cu/MgB_2 wire and YSZ coatings with varying thicknesses. It was observed that displacement values are independent from YSZ thicknesses and the maximum effective stress value is in the Cu region. The surface morphologies and microstructure of samples were characterized using SEM. SEM micrographs of the insulation coatings revealed cracks, pinholes and mosaic structure.

1. Introduction

In the last few years, many groups fabricated MgB_2 wires using powder in-tube process for long length applications such as transformer, generator, solenoids, the Magnetic Resonance Imaging (MRI) and racetrack coils [1–3]. Numerous efforts to develop MgB_2 coils are ongoing. Two techniques "Wind and React" (W&R) and "React and Wind" (R&W) have been used for coil application. Especially (W&R), technique has been used for small radius of MgB_2 coils where the weight is a concern. Several insulators are used to fabricate coils and magnets and there is a relation between the choice of insulating material and the production of coil. In (W&R) technique, the most commonly used insulation is obtained from S-glass and sol–gel ceramic coating [4–6].

The most promising method for insulation coating is the reel-to-reel, continuous sol–gel technique. The National High Magnetic Field Laboratory (NHMFL) developed this technique to provide turn-to-turn electrical insulation for high temperature superconductor (HTS) and low temperature superconductors (LTS) coil [7–10]. In literature, many studies concerning with the physical and mechanical properties of insulators are available, but very few are related with the residual stress, which suffer from failure due to flaking and cracking because of the thermal and elastic mismatch, the plastic flow stress of the metal, the relative substrate coating thickness, thickness of interlayers and fracture resistance of the interface. Moreover, failures in sol–gel coatings depend on processing parameters [11]. The residual stresses can be computed using many different methods, such as numerical, analytical, hole drilling, layer removal, curvature, displacement, fracture, strain, neutron and X-ray diffraction methods.

The aim of the present work is to investigate the residual stresses which occur for the long length, homogeneous YSZ insulation coating on axially symmetric CTFF Cu/MgB_2 wires for W&R MgB_2 coils. The residual stresses, which arise during the coating process due to cooling from formation temperature to room temperature, can cause the crack formations and failures. In the current study, the effect of thickness of the YSZ coatings on the residual stress is calculated for the YSZ coated CTFF Cu/MgB_2 wires.

2. Experimental procedure

2.1. Preparation and coating of YSZ on Cu/MgB_2 wires

The monofilament MgB_2 wires were fabricated using the CTFF process by Hyper Tech Research Inc. MgB_2 wires were manufactured from pure Mg and B powder with the stochiometric composition. CTFF is essentially an in situ PIT method without the long mechanical/thermo-mechanical processes. It can be found more information for CTTF process in Refs. [12,13]. Diameter of the Cu/MgB_2 wires was 1.03 mm and

* Corresponding author. Tel.: +90 212 3810323; fax: +90 212 3810000.
E-mail address: lutfi.arda@bahcesehir.edu.tr (L. Arda).

0925-8388/$ – see front matter © 2008 Elsevier B.V. All rights reserved.
doi:10.1016/j.jallcom.2008.02.080

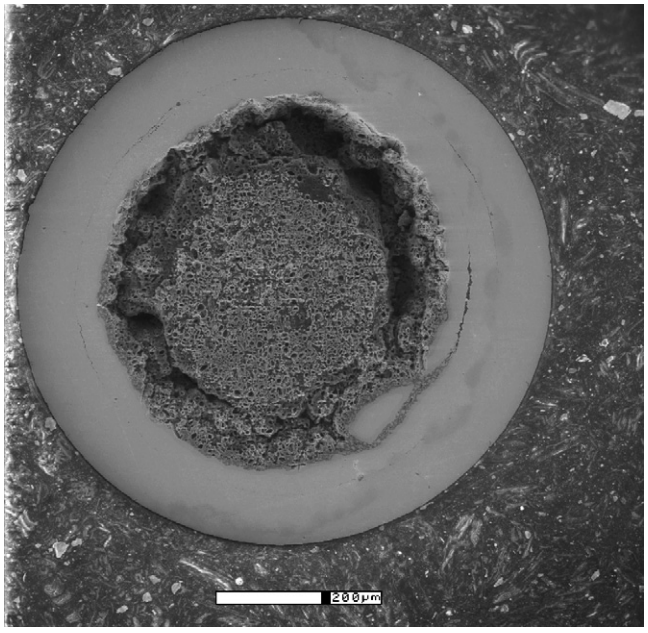

Fig. 1. Typical SEM micrographs of cross section area of Cu/MgB_2 wire. The white scale bar is 200 μm.

the cross-sectional areas of superconducting cores were found to be 2.9×10^{-3} cm^2 from SEM picture as shown in Fig. 1.

The 3 mol% Y_2O_3–ZrO_2 solutions were synthesized by sol–gel process using Yttrium acetate and Zirconium tetrabutoxide. Yttrium acetate 99.99% was dissolved in isoproponal at room temperature by stirring for 90 min. $Zr[O(CH_2)_3CH_3]_4$ was then added. Glacial acetic acid (GAA) and Acetyl acetone were used as chelating agent in solution, and then mixed with a magnetic stirrer for 24 h at room temperature until a transparent solution was obtained just like Ref. [11]. The pH of the solution was measured by standard pH meter. Isoproponal was used to vary viscosity of the solutions.

YSZ film was coated on Cu/MgB_2 wires with sol–gel method by using vertical three-zone furnace as seen in Fig. 2. Furnace zone temperatures were between 450 and 700 °C from bottom to the top. The film thickness was controlled by the withdrawal speed, the number of dipping and the viscidity of the solution.

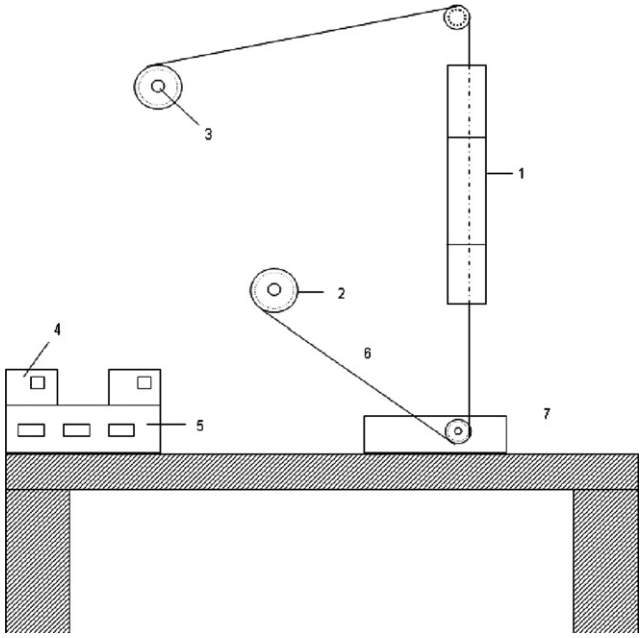

Fig. 2. The continuous, reel-to-reel sol–gel coating system; (1) a three-zone-furnace, (2) pay-off spool, (3) take-up spool, (4) two electric motor for spool, (5) furnace controllers, (6) tapes or wire being insulated and (7) solution tank.

Table 1
Properties of the Materials [14–17]

	Index number	E (GPa)	ν	α (10^{-6} K)
MgB_2	1	151	0.18	8.3
Cu	2	120	0.32	16.7
YSZ	3	53	0.25	7.2

Table 2
Dimensions of the Structure as μm

	Case I	Case II	Case III
b	309	309	309
c	515	515	515
d	516	517	518

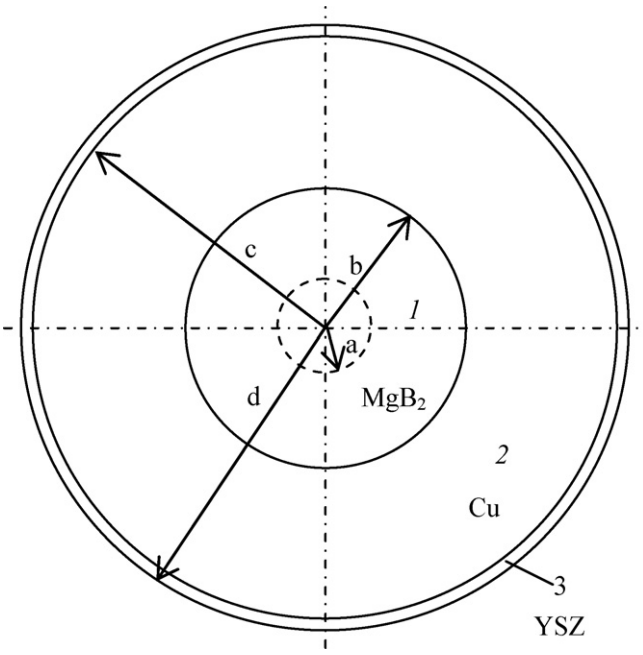

Fig. 3. Sketch of axially symmetric $YSZ/Cu/MgB_2$ wire.

Cu/MgB_2 wires were insulated, and it was verified that the sol–gel insulation coating process did not affect the superconducting properties. Surface morphology, thickness and stochiometry of coating films were observed by using the Environmental Scanning Electron Microscope (SEM, electro scan model E-3), the Tencor Alpha-step 200 profilemeter, and the Energy Dispersive Spectroscopy (EDS), respectively.

2.2. Residual stress analysis of axially symmetric $YSZ/Cu/MgB_2$ wires

In this section, the residual stress is examined in axially symmetric $YSZ/Cu/MgB_2$ wires. Material properties at room temperature, and the dimensions of the investigated sample are given in Tables 1 and 2, respectively.

Lamé's solution [18] can be used to calculate the stress state in this cylindrical rod which is composed of ($YSZ/Cu/MgB_2$). The materials filling the regions in the structure are indexed as shown in Fig. 3.

The related solution of the problem is obtained using continuity conditions among the regions of structure. They are as follows:

(1) Displacement between the region in the centre, indexed by 1 and the second region, indexed by 2

$$u_1 = u_2 \quad \text{at} \quad r = b \tag{1}$$

and

(2) Displacement between the second region, indexed by 2 and the third region (YSZ coating), indexed by 3

$$u_2 = u_3 \quad \text{at} \quad r = c \tag{2}$$

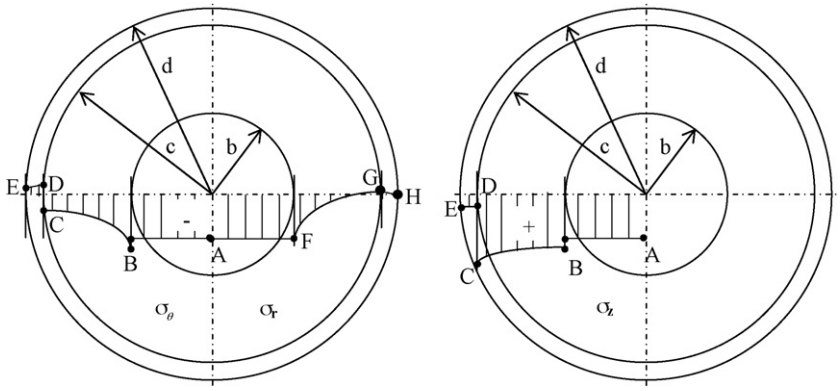

Fig. 4. Variations of stress components, σ_r, σ_θ, σ_z.

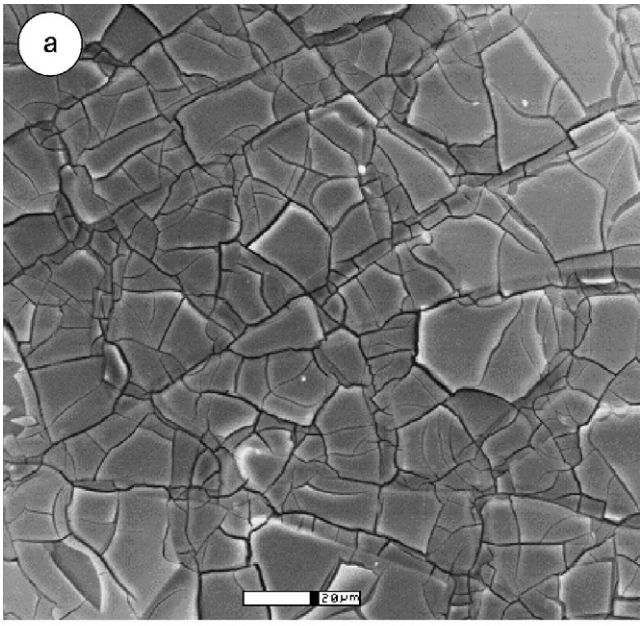

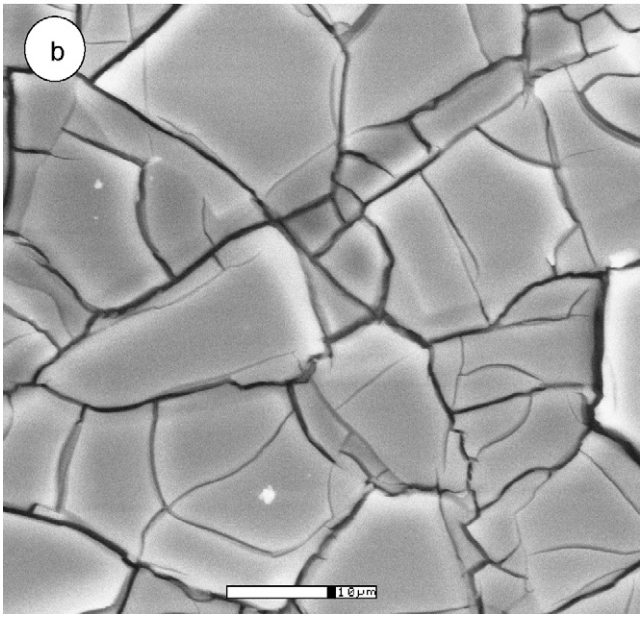

Fig. 5. Typical SEM micrographs of the surface of sol–gel insulated Cu/MgB_2 wire. The scale bar are 20 μm, and 10 μm, in (a) and (b) respectively.

According to Lamé's solution, the expression of displacement is

$$u = \frac{1-2\nu}{E}\frac{p_i r_i^2 - p_o r_o^2}{r_o^2 - r_i^2} r + \frac{1+\nu}{E}\frac{r_i^2 r_o^2}{r}\frac{p_i - p_o}{r_o^2 - r_i^2} \tag{3}$$

where ν and E denote the Poisson's ratio and modulus of elasticity, respectively. r_i and r_o represent the inner and outer radii of the cylinder, and p_i and p_o are the uniform internal and external pressures acting on the boundaries.

If Eq. (3) is written for both of the first and second conditions given above, the following expressions are obtained.

$$\frac{1-2\nu_1}{E_1} p_b b + b\alpha_1 \Delta T = -\frac{1-2\nu_2}{E_2}\frac{p_b b^2 + p_c c^2}{c^2 - b^2} b - \frac{1+\nu_2}{E_2} bc^2 \frac{p_b + p_c}{c^2 - b^2} + b\alpha_2 \Delta T \tag{4}$$

$$-\frac{1-2\nu_2}{E_2}\frac{p_b b^2 + p_c c^2}{c^2 - b^2} c - \frac{1+\nu_2}{E_2} b^2 c \frac{p_b + p_c}{c^2 - b^2} + b\alpha_2 \Delta T = \frac{1-2\nu_3}{E_3}\frac{p_c}{d^2 - c^2} c^3 + \frac{1+\nu_3}{E_3} cd^2 \frac{p_c}{d^2 - c^2} + c\alpha_3 \Delta T \tag{5}$$

where αi (i = 1, 2 and 3) is the thermal expansion coefficient belong to the associated material and ΔT is the difference of temperature. It should be noted that the formulation mentioned above is valid for plane stress. Therefore, Poisson's ratio, modulus of elasticity and the thermal expansion coefficient should be substituted in the formulations as $\nu/(1-\nu)$, $E/(1-\nu 2)$ and $\alpha/(1+\nu)$ for plane strain solution, respectively. The simultaneous solution of Eqs. (4) and (5) gives the radial stresses among the regions, represented by p_b and p_c, that occur during the cooling process. Radial and circumferential stress components can be calculated in the parts of the relevant structure using Lamé's stress formulation given below because p_b and p_c are already obtained values.

$$\sigma_r = \frac{r_i^2 r_o^2 (p_o - p_i)}{r_o^2 - r_i^2}\frac{1}{r^2} + \frac{p_i r_i^2 - p_o r_o^2}{r_o^2 - r_i^2} \tag{6}$$

$$\sigma_\theta = -\frac{r_i^2 r_o^2 (p_o - p_i)}{r_o^2 - r_i^2}\frac{1}{r^2} + \frac{p_i r_i^2 - p_o r_o^2}{r_o^2 - r_i^2} \tag{7}$$

$$\sigma_z = \nu(\sigma_r + \sigma_\theta) - \alpha E \Delta T \tag{8}$$

where σ_z is the stress component along the length. The obtained values are given below for Case I, II, and III, which are 1, 2 and 3 μm of YSZ thicknesses, respectively.

2.2.1. Case I

The p_b and p_c are obtained as −394.3 and 0.071 MPa, respectively. The displacements are obtained as −2.48 and −3.3 μm where r = 309 μm and r = 515 μm, respectively. Values of stress components, σ_r, σ_θ, and σ_z, illustrated in Fig. 4, are given for different points in Table 3.

2.2.2. Case II

The p_b and p_c are obtained as −394.4 and 0.14 MPa, respectively. The displacements are obtained as −2.48 and −3.3 μm where r = 309 μm and r = 515 μm, respectively. Values of stress components, σ_r and σ_θ, illustrated in Fig. 4, are given for different points in Table 3.

2.2.3. Case III

The p_b and p_c are obtained as −394.4 and 0.21 MPa, respectively. The displacements are obtained as −2.48 and −3.3 μm where r = 309 μm and r = 515 μm, respectively. Values of stress components, σ_r and σ_θ, illustrated in Fig. 4, are given for different points in Table 3.

We also calculated for the YSZ insulating coating thickness as 10 μm in order to see the effect of the insulating coating thickness on the residual stress. It was computed that displacement values stay nearly constant, as well, variation of stress component values.

Table 3
Variation of stress components (MPa)

	σ_θ				
Points	A	B	C	D	E
Case I	−394.3	−838.2	−443.8	36.76	36.68
Case II	−394.4	−838.5	−444	36.65	36.5
Case III	−394.4	−838.9	−444.2	36.54	36.33

	σ_r			
Points	A	F	G	H
Case I	−394.3	−394.3	0.071	0
Case II	−394.4	−394.4	0.14	0
Case III	−394.4	−394.4	0.21	0

	σ_z				
Points	A	B	C	D	E
Case I	706.53	962.30	1214.71	267.55	267.51
Case II	706.50	962.18	1214.67	267.54	267.46
Case III	706.50	962.05	1214.63	267.53	267.42

Table 4
Ratios of the stress components for interlayers

	$\left\lvert\frac{\sigma_\theta(\mathrm{Cu})}{\sigma_\theta(\mathrm{MgB_2})}\right\rvert$	$\left\lvert\frac{\sigma_\theta(\mathrm{Cu})}{\sigma_\theta(\mathrm{YSZ})}\right\rvert$	$\left\lvert\frac{\sigma_z(\mathrm{Cu})}{\sigma_z(\mathrm{MgB_2})}\right\rvert$	$\left\lvert\frac{\sigma_z(\mathrm{Cu})}{\sigma_z(\mathrm{YSZ})}\right\rvert$
Case I	2.126	12.073	1.362	4.54
Case II	2.126	12.115	1.361	4.54
Case III	2.127	12.157	1.361	4.54

3. Results and discussion

YSZ insulation coatings were deposited on Cu/MgB_2 wires with various dip numbers by the reel-to-reel sol–gel process. After coating, the samples of $YSZ/Cu/MgB_2$ strand were annealed at 700 °C for 30 min with 5.8 °C/min heating rate under 4% H_2–Ar gas flow. Thickness of YSZ insulation coatings, about 1, 2 and 3 μm, uniform along the samples, is determined using SEM. SEM observation indicates that YSZ coatings have cracks, pinholes and mosaic structure, which is desired in ceramic insulators as shown in Fig. 5a and b. However these cracks are decreasing with reducing thickness.

There are a lot of numerical, analytical and experimental works on this subject [19–21]. Thermal stress analysis of YSZ insulation on Cu/MgB_2 wire was analytically investigated as a function of YSZ coating thickness. Stress components were calculated using axially symmetric Cu/MgB_2 wires which were coated with various thicknesses of YSZ insulation. It is interesting of evaluating the stress components in the interfaces due to their discontinuity and extreme values. It was found that displacements are independent from YSZ coating thicknesses. The used formulation in the solution is belonged to Lamé and, for this formulation, p_a is equal to zero in the presented problem in all cases, p_b was found nearly constant in all cases but magnitude of p_c increased with thickness of YSZ. Moreover p_b was in compression while p_c was in tension in all cases.

Circumferential stress components are in tension in the YSZ insulation region. The other regions were under compression. Maximum circumferential stress component value was obtained at point B, illustrated in Fig. 4, in the copper region. The maximum compression value exhibited a small increase with the thicknesses of YSZ insulation. The minimum value of circumferential stress component was obtained in point E, illustrated in Fig. 4, in the region of YSZ as tension. The stress component values of YSZ region exhibited a small decrease with the thicknesses of insulation coating.

Radial stress components were in compression and remain to be constant in the region of MgB_2 for all cases. In the copper region, radial stress component changed sign and went to zero in the outer surface.

The axial stress component, σ_z, was in tension in all cases and reached its maximum value at point C, illustrated in Fig. 4, in the copper region, minimum value was in the outer surface. As shown in Fig. 4 and Table 3, the critical region is copper. σ_z and σ_θ have a discontinuity in both interlayers MgB_2 to Cu and Cu to YSZ, however, radial component has no discontinuity (Table 4).

4. Conclusions

YSZ coatings on Cu/MgB_2 wires were fabricated by the reel-to-reel sol–gel process for W&R MgB_2 Coil. SEM micrographs of the insulation coating revealed cracks, pinholes and mosaic structure which is desired for the adhesion of final protecting epoxy layer in W&R MgB_2 Coil.

Residual stress analysis of YSZ insulation coating on Cu/MgB_2 wires is investigated varying thicknesses using Lamé's formulation in axially symmetric structure. It is observed that the effect of thicknesses of YSZ insulation coatings on residual stress can be neglected.

Maximum circumferential stress component value was obtained as −838.9 MPa at point B, in the copper region. The radial displacements values remain to be constant for increasing insulation coating thicknesses.

Acknowledgments

The author (L. Arda) thanks Dr. Y.S. Hascicek and M. Tomsic at CEO, IEMM Inc. and Hyper Tech Research Inc., for providing MgB_2 wires and chemical materials.

References

[1] M.D. Sumption, M. Bhatia, M. Rindfleisch, J. Phillips, M. Tomsic, E.W. Collings, IEEE Trans. Appl. Superconduct. 15 (2005) 1457–1460.
[2] M.D. Sumption, M. Bhatia, F. Buta, S. Bohnenstiehl, M. Tomsic, M. Rindfleisch, J. Yue, J. Phillips, S. Kawabata, E.W. Collings, Supercond. Sci. Technol. 18 (2005) 961–965.
[3] L. Arda, O.A. Sacli, M. Tomsic, O. Dur, Y.S. Hascicek, Supercond. Sci. Technol. 20 (2007) 1054–1058.
[4] M.D. Sumption, S. Bohnenstiehl, F. Buta, M. Majoros, S. Kawabata, M. Tomsic, M. Rindfleisch, J. Phillips, J. Yue, E.W. Collings, IEEE Trans. Appl. Super. 17 (2007) 2286–2289.
[5] M.D. Sumption, M. Bhatia, F. Buta, S. Bohnenstiehl, M. Tomsic, M. Rindfleisch, J. Yue, J. Phillips, S. Kawabata, E.W. Collings, Phys. C 458 (2007) 12–20.
[6] Y.S. Hascicek, Z. Aslanoglu, L. Arda, Y. Akin, M.D. Sumption, M. Tomsic, Adv. Cryog. Eng. Mater. 50 (2004) 541–545.
[7] E. Celik, H. I. Mutlu, Y.S. Hascicek, US Patent No: 6,344,287 (2002).
[8] O. Cakiroglu, L. Arda, Y.S. Hascicek, Phys. C 422 (2005) 117–126.
[9] O. Cakiroglu, L. Arda, Z. Aslanoglu, Y. Akin, O. Dur, A. Kaplan, Y.S. Hascicek, Adv. Cryog. Eng. 711 (2004) 184–192.
[10] E. Celik, Y. Akin, I.H. Mutlu, W. Sigmund, Y.S. Hascicek, Phys. C 382 (2002) 355–360.
[11] L. Arda, S. Ataoglu, S. Sezer, Z. Abdulaliyev, Surf. Coat. Tech. 202 (2007) 439–446.
[12] E.W. Collings, E. Lee, M.D. Sumption, M.X. Tomsic, L. Wang, S. Soltanian, S.X. Dou, Phys. C 386 (2003) 555–559.
[13] M. Tomsic, M. Rindfleisch, J. Yue, K. McFadden, D. Doll, J. Phillips, M.D. Sumption, M. Bhatia, S. Bohnenstiehl, E.W. Collings, Phys. C 456 (2007) 203–208.
[14] W. Goldacker, S.I. Schlachter, S. Zimmer, H. Reiner, Supercond. Sci. Technol. 14 (2001) 787–793.
[15] P. Kovac, M. Dhalle, T. Melisek, H.J.N. van Eck, W.A.J. Wessel, B. ten Haken, I. Husek, Supercond. Sci. Technol. 16 (2003) 600–607.
[16] M. Mogensen, N.M. Sammes, G.A. Tompsett, Solid State Ion. 129 (2000) 63–94.
[17] K. Dai, L. Shaw, Acta Mater. 52 (2004) 69–80.
[18] S.P. Timoshenko, J.N. Goodier, Theory of Elasticity, McGraw-Hill, New York, 1970.
[19] X.C. Zhang, B.S. Xu, H.D. Wang, Y.X. Wu, Thin Solid Films 488 (2005) 274–282.
[20] X.C. Zhang, J.M. Gong, S.D. Tu, J. Mater. Sci. Technol. 20 (2004) 149–153.
[21] Y.H. Yu, M.O. Lai, L. Lu, P. Yang, J. Alloy. Compd. 449 (2008) 56–59.